J Solid State Electrochem (2011) 15:473–478
DOI 10.1007/s10008-010-1107-8

ORIGINAL PAPER

A soft chemistry synthetic method for preparing $LiNi_{0.8}Co_{0.2}O_2$ with enhanced electrochemical performances

Xiaoyu Cao · Lingling Xie · Ruijuan Wang

Received: 1 May 2010 / Accepted: 4 May 2010 / Published online: 26 May 2010

Abstract Polycrystalline $LiNi_{0.8}Co_{0.2}O_2$ powders were synthesized via the citric acid-assisted liquid phase evaporation method. The precursors are homogenously mixed in the solutions at an atomic scale which is also reflected by the particle distribution of the final products. The optimal synthesis temperature is located at 750 °C where the particle size, crystalline structure, and the cation disorder between Li^+ and Ni^{2+} ions have been balanced. A high discharge capacity of 191 mAh g^{-1} (3.0–4.3 V at 30 mA/g) is achieved in the first cycle for the 750 °C-prepared sample with a capacity retention of 89.37% after 96 cycles. Cyclic voltammetry and the differential capacity curves also reveal a moderate stable crystal structure of 750 °C-prepared $LiNi_{0.8}Co_{0.2}O_2$ during the prolonged cycles.

Keywords Soft chemistry synthesis · $LiNi_{0.8}Co_{0.2}O_2$ · Cathode material · Lithium ion batteries · Electrochemical performances

Introduction

Over the past years, the demand for lithium ion batteries with excellent electrochemical performances has grown tremendously due to the development and popularity of portable electronic devices such as PDA, cellular phone, and laptop computers. The utilization of Li ion batteries in the large-scale application such as electric vehicles and hybrid electric vehicles makes it important to further improve the existing cathode materials in terms of energy density, stability, safety, and cost. Of the various cathode materials, layered $LiNi_{1-x}Co_xO_2$ ($0<x1$) systems have been extensively studied and identified as one of the most attractive materials for lithium ion batteries [1–7] considering the cost and electrochemical performances [8–13].

Many efforts are devoted to the development of a high-performance $LiNi_{0.8}Co_{0.2}O_2$ cathode material. At present, the studies concerning the $LiNi_{0.8}Co_{0.2}O_2$ can be categorized into two different explorative categories. One is to employ novel synthesis routes such as the controlled crystallization method [8], the organic acid-assisted synthesis method [9, 10], the emulsion drying method [11], the Ni–Co hydroxide–carbonate precursor method [12], and the polymer–pyrolysis method [13] to prepare $LiNi_{0.8}Co_{0.2}O_2$ with good electrochemical activity. These synthesis reactions are usually carried out under a mild condition because of the preparation of the homogeneous precursors. Well-developed layered structure and well-controlled morphology of $LiNi_{0.8}Co_{0.2}O_2$ particles are usually obtained in those aforementioned approaches at a relatively low temperature with a shortened dwell time and exhibiting improved electrochemical performances. The other investigation direction for $LiNi_{0.8}Co_{0.2}O_2$ includes the modifications on $LiNi_{0.8}Co_{0.2}O_2$ compositions such as partially substituting for Li or Ni or Co with the different doping elements [14–19] or surface coating by electrochemically inactive compounds [20–24] to attain a stable capacity retention and satisfactory thermal stability.

However, the electrochemical performances of the electrode materials highly depend on the structural and particle size characters of the host cathode materials [13]. For $LiNi_{0.8}Co_{0.2}O_2$, a key problem is how to prepare a

Presented at the 60th Annual ISE Meeting on Electrochemical Energy Conversion and Storage, Beijing, People's Republic of China, August 16–21, 2009

X. Cao (✉) · L. Xie · R. Wang
School of Chemistry and Chemical Engineering,
Henan University of Technology,
Zhengzhou 450001, People's Republic of China
e-mail: caoxy@haut.edu.cn

more orderly layered compound with desirable particle size distribution, which has an immediate impact on its final electrochemical performances. Thus, an optimized synthesis method is very important for the utilization of high-performance $LiNi_{0.8}Co_{0.2}O_2$. Herein, a novel soft chemistry synthesis technique is reported to successfully prepare polycrystalline $LiNi_{0.8}Co_{0.2}O_2$ powders with the improved electrochemical performances. This process starts from mixed solutions containing citric acid in which the solid particles and liquid substances were uniformly distributed. The structural evolution and the particle size distribution are correlated with the electrochemical behaviors of the as-synthesized $LiNi_{0.8}Co_{0.2}O_2$ in detail.

Experimental

Layered $LiNi_{0.8}Co_{0.2}O_2$ powders were synthesized by the citric acid-assisted liquid phase evaporation method. $LiOH{\cdot}H_2O$, $Ni(NO_3)_2{\cdot}6H_2O$, $Co(NO_3)_2{\cdot}6H_2O$ and $C_6H_8O_7{\cdot}H_2O$ were dissolved in distilled water, in the molar ratio of 5:4:1:5. Citric acid was used as the complexing agent. Then, the three solutions were mixed and evaporated until the slurry residue was obtained. Afterwards, the slurry was allowed to dry at 110 °C followed by grinding, which gave rise to a powder, referred to as the $LiNi_{0.8}Co_{0.2}O_2$ precursor. Lastly, the precursor was heated in SK_2 tube-type furnace (Zhonghuan, Tianjin) at 700–800 °C in an oxygen atmosphere for 10 h to obtain the polycrystalline $LiNi_{0.8}Co_{0.2}O_2$ powders.

Powder X-ray diffraction (XRD) analysis using CoKα radiation (λ=1.78901 Å) was employed to identify the crystalline phase of the as-prepared powders on XRD-Pert Pro diffractometer (XPERT PRO MPD, Netherlands) in the range of $10°\leq 2\theta \leq 90°$. The laser particle size distribution was calculated on Malvern Mastersizer-2000 (Malvern instruments, England) using a laser granulometer based on a laser wavelength of 830 nm, power of 3 mW, and a multielement 42-channel detector. The as-synthesized powders were mixed with 10% acetylene black and 10% polytetrafluoroethylene and used as cathode while lithium foil disks were used as anode in the CR-2016 coin cells. The electrolyte was prepared by mixing 1 M $LiClO_4$ in a 1:1 (*v*/*v*) mixture of ethylene carbonate and dimethyl carbonate solution (Guotai-Huarong, Zhangjiagang). An aluminum mesh acted as the current collector. Celgard-2400 membrane was used as the cell separator. The charge/discharge data were collected using CT-3008 W-5V5mA-S4 Neware battery tester (Neware, Shenzhen) at ambient temperature within the potential range of 3.0–4.3 V at a current rate of 30 mA g^{-1}. Cyclic voltammetric studies were performed with lithium metal foil counter and reference electrodes. Cyclic voltammograms (CV) were run on a CHI660 electrochemical workstation (Chenhua, Shanghai) at a scan speed of 50 μV s^{-1}.

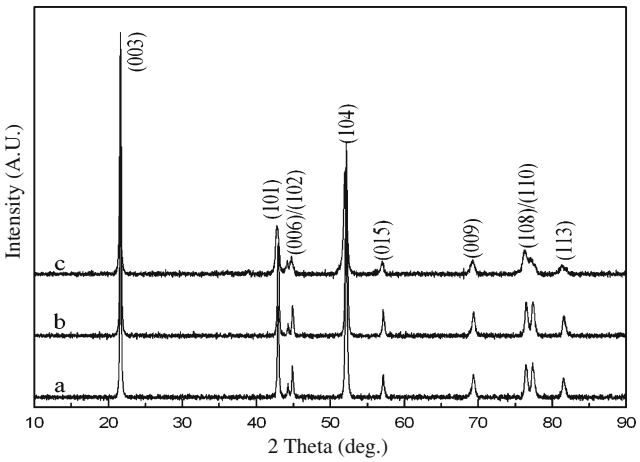

Fig. 1 XRD patterns of $LiNi_{0.8}Co_{0.2}O_2$ powders obtained at different temperatures: **a** 700 °C, **b** 750 °C, **c** 800 °C

Results and discussion

Figure 1 shows the XRD patterns of the $LiNi_{0.8}Co_{0.2}O_2$ powders heated at different temperatures. The XRD patterns of $LiNi_{0.8}Co_{0.2}O_2$ powders show a well-defined peak at about 2θ=21.7° and the other less intensity peaks at about 42.9° and 52.1°. All the diffraction peaks are indexed to the layered α-$NaFeO_2$ structure with the $R\bar{3}m$ space group. The main Bragg diffraction peaks for the material are labeled with (*hkl*) indexes. In addition, a clear splitting of the (006)/(102) and (108)/(110) doublets are observed for the powders obtained at 700 °C and 750 °C. As the calcination temperature is increased to 800 °C, (006)/(102) and (108)/(110) doublets tend to merge into a single peak. According to references [25–27], the splitting degree of the doublets (006)/(102) and (108)/(110), as well as the ratios of *c*/*a* and $I_{(003)}/I_{(104)}$, has been considered as a qualitative measure to judge the structural ordering of the materials. The higher the ratios of *c*/*a* and $I_{(003)}/I_{(104)}$ of a material, the higher the hexagonal ordering is. At the same time, the lower *R*-factor which is defined as $[I_{(006)}+I_{(102)}]/I_{(101)}$ and

Table 1 Structural and lattice parameters for $LiNi_{0.8}Co_{0.2}O_2$ powders obtained at different temperatures for 10 h

Powders	*a* (Å)	*c* (Å)	*c*/*a*	Unit cell volume (Å^3)	$I_{(003)}/I_{(104)}$	*R*-factor
700 °C	2.8576	14.1863	4.9644	100.3264	1.535	0.442
750 °C	2.8560	14.1885	4.9680	100.2302	1.538	0.452
800 °C	2.8632	14.1812	4.9530	100.6801	1.506	0.703

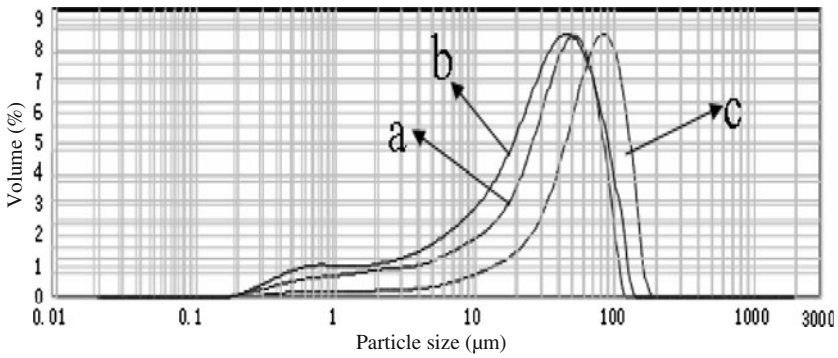

Fig. 2 Particle size distribution curves of $LiNi_{0.8}Co_{0.2}O_2$ powders obtained at different temperatures: **a** 700 °C, **b** 750 °C, **c** 800 °C

the smaller hexagonal unit cell volume are also regarded as a good indicator of hexagonal ordering of the system [28, 29]. Table 1 presents the structural and lattice parameters for $LiNi_{0.8}Co_{0.2}O_2$ powders obtained at different temperatures for 10 h. As shown in Table 1, $LiNi_{0.8}Co_{0.2}O_2$ powder made at 750 °C displays the maximal ratios of *c/a* and $I_{(003)}/I_{(104)}$ and the minimal unit cell volume, indicating a more orderly layered structure. For the powder obtained at 700 °C, the *R*-factor attained the minimal value of 0.442. However, $LiNi_{0.8}Co_{0.2}O_2$ powder prepared at 800 °C exhibits the lowest ratios of *c/a* and $I_{(003)}/I_{(104)}$, the largest unit cell volume and the highest *R*-factor, which implies a severe cation mixing and formation of the $[Li_{1-x}Ni_x^{2+}]$ $[(Ni_{1-x}^{3+}\ Ni_x^{2+})_{0.8}Co_{0.2}]O_2$ formula in the high calcination temperature. This can be assigned to the lithium deficiency in the 800 °C product since more lithium source in the precursor may evaporate at higher temperatures and lithium content also significantly influences the cation disorder between Li^+ and Ni^{2+} ions.

Figure 2 shows the particle size distribution of as-prepared $LiNi_{0.8}Co_{0.2}O_2$. It displays the variation concerning volume fraction of the particle with the particle size. As indicated in Fig. 2, all the powders are characterized by a large volume distribution resulting from one population and exhibit a characteristic of normal distribution. The selected particle size distribution data of $LiNi_{0.8}Co_{0.2}O_2$ powders are listed in Table 2 along with a summary of specific surface areas. D_{50}, which is also called as the volume median diameter of particles,

Table 2 Particle size distribution and specific surface area of $LiNi_{0.8}Co_{0.2}O_2$ powders obtained at different temperatures

Powders	D_{10} (μm)	D_{50} (μm)	D_{90} (μm)	Specific surface area ($m^2 g^{-1}$)
700 °C	2.808	34.374	74.796	0.993
750 °C	2.331	29.607	78.439	1.14
800 °C	15.974	65.770	120.609	0.337

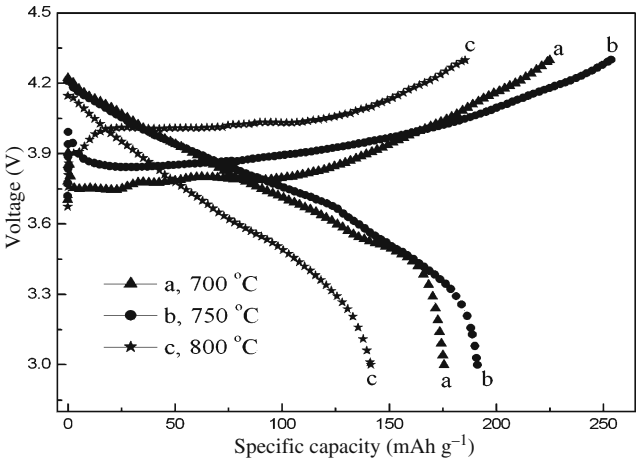

Fig. 3 The first charge–discharge curves of $LiNi_{0.8}Co_{0.2}O_2$ powders treated at different temperatures for 10 h

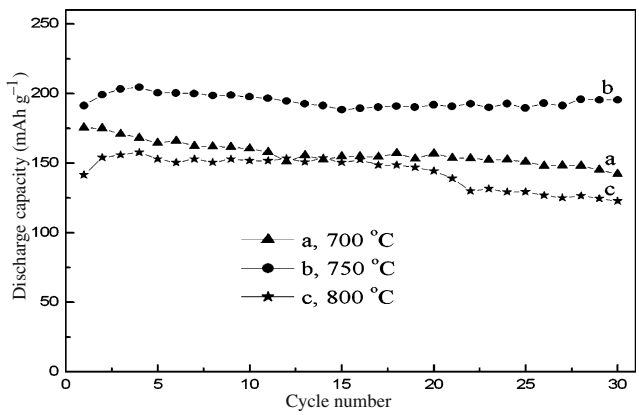

Fig. 4 Discharge capacity vs. cycle number curves of $LiNi_{0.8}Co_{0.2}O_2$ powders prepared at various temperatures for 10 h

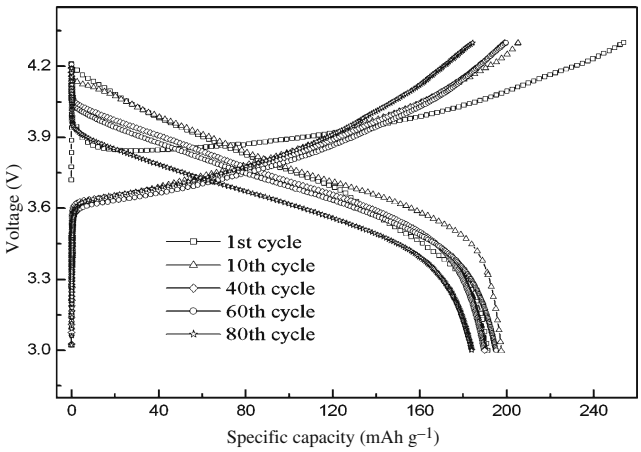

Fig. 5 The selected charge/discharge curves of $LiNi_{0.8}Co_{0.2}O_2$ powder heated at 750°C for 10 h

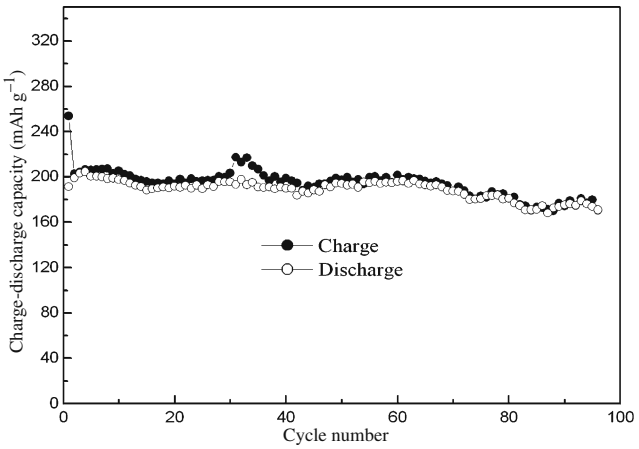

Fig. 7 Variation of charge/discharge capacity vs. number of cycles using the $LiNi_{0.8}Co_{0.2}O_2$ powder heated at 750°C for 10 h

denotes the maximal particle size when the volume ratio of the cumulative volume to total volume equals to 50%. The meaning of D_{10} and D_{90} can be analogical. The volume median diameters of particles (D_{50}) for the three powders annealed at 700°C, 750°C, and 800°C are 34.374, 29.607, and 65.770 μm, respectively, whereas the specific surface areas for the three powders are 0.993, 1.140, and 0.337 $m^2 g^{-1}$. The results reveal that the 750°C-synthesized product has a smaller and a more uniformly distributed particle size than those of the other two samples. According to Yang et al. [12], polycrystalline $LiNi_{0.8}Co_{0.2}O_2$ can be formed at about 726°C via a soft chemistry synthesis route by employing $LiOH{\cdot}H_2O$, $Ni(NO_3)_2{\cdot}6H_2O$, and $Co(NO_3)_2{\cdot}6H_2O$ as the starting materials. Thus, 750°C may be a transition temperature associated with the change of the particle size. Further increasing the calcination temperature to 800°C increases the particle size, which contributes to the decreased specific surface area of the powder. In general, a large surface area is beneficial with respect to the delivery of the high discharge capacity. Because the intercalation process of Li^+ ion into the cathode materials is often a diffusion-controlled progress, so the particle characteristics of 750°C-synthesized powder may facilitate electrolyte soaking into particles and shorten the diffusion distance of Li^+ ion, which accordingly improves the diffusion kinetics of Li^+ into/out of $LiNi_{0.8}Co_{0.2}O_2$ electrode.

Fig. 6 Cycling voltammograms of $LiNi_{0.8}Co_{0.2}O_2$ powder calcined at 750°C for 10 h

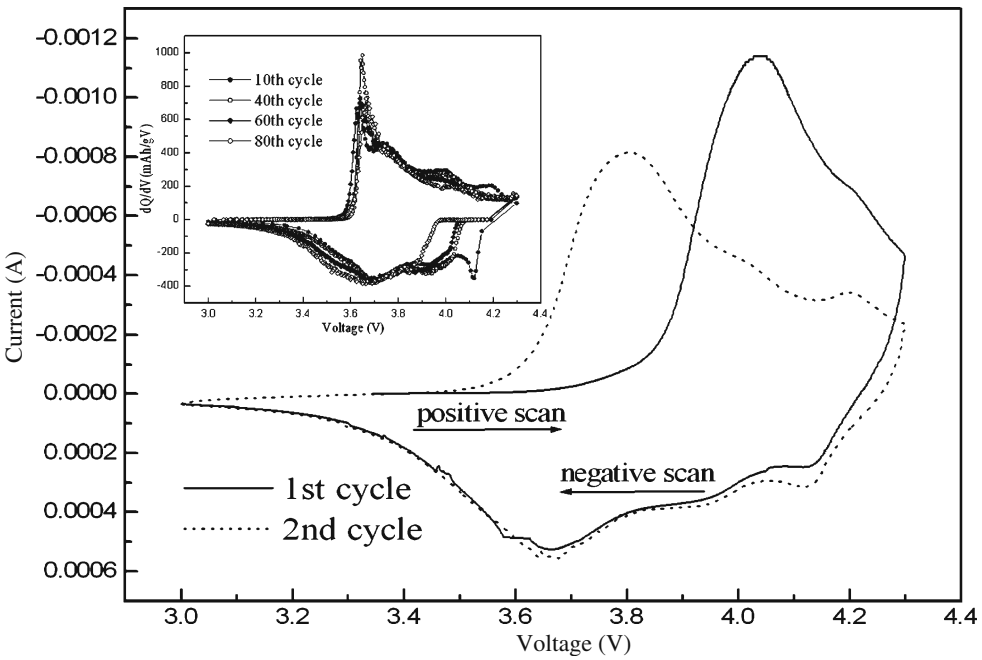

Figure 3 shows the first charge/discharge curves of $LiNi_{0.8}Co_{0.2}O_2$ powders treated at different temperatures. Among the three samples, the one prepared at 750 °C demonstrates the highest charge/discharge capacities of 253.9/191.3 mAh g^{-1}, respectively. Moreover, it is clearly observed that the discharge plateau of the 750 °C-synthesized powder is higher than those of the other two, suggesting a decreased electrode polarization during the discharge process. Cycle-life plots of $LiNi_{0.8}Co_{0.2}O_2$ powders prepared at different temperatures for 10 h are illustrated in Fig. 4. The capacity fading rates within 30 cycles are 18.77%, 1.85%, and 20.26% for the three samples prepared at 700 °C, 750 °C, and 800 °C, respectively. Obviously, at 750 °C, the cation disorder and the particle morphology of the $LiNi_{0.8}Co_{0.2}O_2$ sample have been balanced very well, favoring its final electrochemical performances. Although the *R*-factor is lowest for 700 °C-synthesized powder, both the *c/a* and $I_{(003)}/I_{(104)}$ ratios are lower and the unit cell volume is larger than those of 750 °C-synthesized powder. In the meantime, 700 °C-synthesized powder has the larger particle size and lower specific surface area, as evidenced in Table 2. From the results obtained so far, it seems that the positive influence factors such as the lowest *R*-factor may be overwhelmed by the negative influence factors such as the lower ratios of *c/a* and $I_{(003)}/I_{(104)}$, larger unit cell volume, and larger particle size for the 700 °C-synthesized powder. As a result, the electrochemical performances of the 700 °C-synthesized powder are inferior to the 750 °C-synthesized powder. When it comes to the powder calcined at 800 °C, it manifests a poor electrochemical activity because of its increased cation mixing and larger particle size.

Figure 5 gives the selected charge/discharge curves of $LiNi_{0.8}Co_{0.2}O_2$ powder heated at 750 °C. It is found that this material delivers a first charge capacity of 253 mAh g^{-1} and discharge capacity of 191 mAh g^{-1} with a coulombic efficiency of 75.3% in the range of 3.0–4.3 V at a current density of 30 mA g^{-1}. Coulombic efficiency keeps above 95% in the subsequent cycles.

Cyclic voltammograms for 750 °C-synthesized powders at a sweep range of 3.0–4.3 V are presented in Fig. 6. For the deintercalation process, there are three oxidation peaks in CV curves. The first board peak is centered at around 4.04 V, corresponding to the phase transition of hexagonal phase to monoclinic phase. However, the remaining two weak peaks at around 4.2 V cannot be very clearly discerned, which represents the phase transition of monoclinic phase to hexagonal phase and hexagonal phase to another hexagonal phase. For the intercalation process, there are three corresponding reduction peaks at 3.68, 3.93, and 4.13 V in CV curves. At the second scan, the three discernable oxidation peaks at 3.80, 4.02, and 4.19 V are observed. It is noticeable that the first oxidation peak at 4.04 V shifts to 3.80 V, indicating a depressed overpotential during Li^+ deintercalation. In order to further understand the structural stability of 750 °C-synthesized powder, the inset in Fig. 6 compares the differential capacity curves on the 10th, 40th, 60th, and 80th cycle. Compared with CV, the differential capacity curves provide a more realistic explanation for the actual state of the cathode material under the galvanostatic cycling [17]. It is observed that the differential capacity curves maintain similar shapes moderately at different cycles though the reduction peaks at about 4.2 V slightly shift to a higher potential.

As a practical electrode cathode material for lithium ion batteries, good cycling stability is an essential and desirable feature. To confirm the electrochemical performance during prolonged cycles, we cycle CR-2016 coin cell incorporating the 750 °C-synthesized powder in the voltage range 3.0–4.3 V at a constant specific current of 30 mA g^{-1}. Excellent cycleability of the material is exhibited by the as-prepared $LiNi_{0.8}Co_{0.2}O_2$ with a capacity loss of only 10.6% after 96 cycles. This enhanced cycleability further confirms that 750 °C is the optimal synthesis temperature for the citric acid-assisted method (Fig. 7).

Conclusion

$LiNi_{0.8}Co_{0.2}O_2$ has been successfully synthesized by the citric acid-assisted liquid phase evaporation process. Due to the advantages of this wet chemistry synthesis method, the powder prepared at 750 °C for 10 h shows a highly ordering of hexagonal layered structure and small average particle size, which contributes to its extraordinary electrochemical performances such as high discharge capacity and excellent cycleability. It yields the initial discharge capacity of 191.3 mAh g^{-1} and remains 89.38% of the original capacity after the 96 cycles. Besides, CV and the differential capacity curves reveal a reversible reactions process after the second cycle. Therefore, the proposed preparation method not only provides an alternative approach to synthesize high performance $LiNi_{0.8}Co_{0.2}O_2$ cathode materials for lithium ion batteries applications but also is feasible to be applied in the preparation of other layered materials with excellent electrochemical performances.

Acknowledgments This research was financially supported by the Zhengzhou Municipal Science and Technology Development Programs (No. 083SGYG25121-3) and Ph.D. Programs Foundation of Henan University of Technology (No. BS2006011).

References

1. Tarascon JM, Armand M (2001) Nature 141:359
2. Whittingham MS (2004) Chem Rev 104:4271

3. Kinoshita A, Yanagida K, Yanai A, Kida Y, Funahashi A, Nohma T, Yonezu I (2001) J Power Sources 102:283
4. Sulaiman MA, Osman Z, Arof AK (2003) J New Mater Electrochem Syst 6:191
5. Wu MQ, Chen A, Xu RQ, Li Y (2003) Mater Sci Eng B 99:336
6. Wang CW, Ma XL, Zhou LQ, Cheng JG, Sun JT, Zhou YH (2007) Electrochim Acta 52:3022
7. Li DC, Peng ZH, Ren HB, Guo WY, Zhou YH (2008) Mater Chem Phys 107:171
8. Ying JR, Wan CR, Jiang CY, Li YX (2001) J Power Sources 99:78
9. Fey GTK, Subramanian V, Lu CZ (2002) Solid State Ion 152–153:83
10. Oh SH, Jeong WT, Cho WI, Cho BW, Woo K (2005) J Power Sources 140:145
11. Cho TH, Chung HT (2005) J Appl Electrochem 35:1033
12. Yang ZX, Wang B, Yang WS, Wei X (2007) Electrochim Acta 52:8069
13. Xiao LF, Yang YY, Zhao YQ, Ai XP, Yang HX, Cao YL (2008) Electrochim Acta 53:3007
14. Wang CW, Ma XL, Cheng JG, Zhou LQ, Sun JT, Zhou YH (2006) Solid State Ion 177:1027
15. Liu L, Su GY, Xiao QZ, Ding YH, Wang CW, Gao DS (2006) Mater Chem Phys 100:236
16. Majumder SB, Nieto S, Katiyar RS (2006) J Power Sources 154:262
17. Oh SH, Lee SM, Cho WI, Cho BW (2006) Electrochim Acta 51:3637
18. Sathiyamoorthi R, Santhosh P, Shakkthivel P, Vasudevan T (2007) J Solid State Electrochem 11:1665
19. Xiang JF, Chang CX, Zhang F, Sun JT (2008) J Electrochem Soc 155:A520
20. Ha HW, Jeong KH, Yun NJ, Hong MZ, Kim K (2005) Electrochim Acta 50:3764
21. Fey GTK, Muralidharan P, Lu CZh, Cho YD (2005) Solid State Ion 176:2759
22. Lee SM, Oh SH, Ahn JP, Cho WI, Jang H (2006) J Power Sources 159:1334
23. Hu GR, Deng XR, Peng ZD, Du K (2008) Electrochim Acta 53:2567
24. Xiang JF, Chang CX, Yuan LJ, Sun JT (2008) Electrochem Commun 10:1360
25. Morales J, Vicente CP, Tirado JL (1990) Mater Res Bull 25:623
26. Ohuzuku T, Ueda A, Nagayama M (1993) J Electrochem Soc 140:1862
27. Choi YM, Pyun SI, Moon SI (1996) Solid State Ion 89:43
28. Reimers JN, Rossen E, Jones CD, Dahn JR (1993) Solid State Ion 61:335
29. Dahn JR, Sacken UV, Michal CA (1990) Solid State Ion 44:87